
CHAPTER 7

Experiment and Results

7.1. Introduction and Aims of the Experiment

In chapter 6, we proposed a novel texture classification scheme that is surface-rotation invariant rather than image-rotation invariant. In this chapter, in order to test the efficiency of the proposed classification scheme for rotation invariant texture analysis, we design and carry out the experimental work on four synthetic textures and thirty real textures.

Regarding the test data set used in the experiment, we note that currently existing and publicly available texture databases are not suitable for our task. In terms of our surface rotation invariant texture classification scheme, the texture database should provide a set of surface rotations rather than image rotations, along with the registered photometric stereo image data. Our developing photometric texture database is not only concerned with the real surface rotation, but also with the different and controlled illuminant conditions. We provide a detailed description of our new photometric texture database contents and measurement procedure. This method gives us enough information about varied images of different kinds of surfaces directly obtained from the surface properties (e.g. surface partial derivative fields). In addition, the database has already been made public and may be used by interested researchers. Our photometric texture database can be accessed and downloaded online from:

<http://www.cee.hw.ac.uk/texturelab/database/>

In this database, images are captured and stored individually while surfaces are rotated and illuminated in varied conditions. In addition, the related settings of the experimental apparatus will be discussed. Thereafter, the experimental processing of photometric stereo is carried out on those images in order to obtain surface partial derivative fields by isolating the albedo information, which will give us the representation of gradient space either in the spatial domain or in the frequency domain. Then, rotation invariant features in polar spectra may be obtained in a straightforward manner. Finally, the classification results on both synthetic textures and real textures will be presented.

7.2. A Photometric Texture Database

7.2.1. Introduction

In order to test the efficiency of the classification scheme proposed in chapter 6, our texture database should provide:

- 1) *real surface rotation* rather than image rotation, where most of currently existing texture databases only support image rotation; and
- 2) *registered photometric stereo data sets* so that we may employ surface properties obtained by photometric stereo in our surface-based classifier.

Therefore, we developed two categories of 3D surface photometric texture databases:

- *Synthetic texture data set*, and
- *Real texture data set*.

where both sets provide a varying range of images of 3D surface texture, captured at different surface rotations and under different controlled illumination conditions so that photometric stereo techniques may be used.

7.2.2. Comparison with Other Existing Texture Databases

There are many texture databases available to the public so far. So-called *Brodatz* textures [Brodatz66] are probably the most widely used image data in the texture analysis literature. Other well known data sets are *CUReT* (Columbia-Utrecht Reflectance and Texture Database, Columbia University) [Dana97] [Dana99a], *VisTex* (Vision Texture Database, MIT) , *MeasTex* (Texture database for the MEASurement of TEXTure classification algorithms, the University of Queensland) [Ohanian92], *OUTex* framework (University of Oulu, Finland) [Ojala96], and *PhoTex* (Texture Lab, Heriot-Watt University) [McGunnigle01], etc.

- *Brodatz Texture Database*

The “*Brodatz* texture database” is derived from the Brodatz album [Brodatz66]. It has a relatively large number of classes (112 classes), and a small number of examples for each class. Although the *Brodatz* texture database has become the standard for evaluating texture algorithms, with hundreds of studies having been applied to small sets of its images, it is not suitable for use by our classification scheme.

Our experiment requires that the photometric stereo algorithms are able to run on textures taken under different and controlled lighting and perspective. Since the *Brodatz* texture database is based on image rotated textures [Leung92] [Greenspan94] [Haley96] [Porter97] [Fountain98] [Ojala00] *et al*, the original *Brodatz* texture database is not suitable for our experiments as it can not provide photometric stereo image sets for each texture classes and it does not provide true surface rotation.

- *VisTex*

To assist in the development of more robust computer vision algorithms and their comparison on a common set of data, the *VisTex* collection has been assembled and maintained by the Vision and Modelling Group at the MIT Media Lab. The most difference between the *VisTex* database and other texture databases is that it does not

conform to *rigid frontal plane perspectives* and *studio lighting conditions*. Their lighting conditions include daylight, artificial-florescent and artificial-incandescent. Moreover, some of the lighting conditions are imprecise. For example, descriptions are given as “*daylight, direct and from right*”. With regard to perspective, the angle between film an object plane, there are two settings: frontal-plain and oblique. Apart from these differences, *VisTex* also provides some examples of many non-traditional textures (such as texture scenes and sequences of temporal textures).

Therefore, considering the limitations of the *VisTex* database with unknown illumination directions, we can not use them with our texture classification scheme, because we have to recover the surface properties from several images with the known and controlled light conditions using photometric stereo.

- ***MeasTex***

MeasTex is about the MEASurement of TEXture classification algorithms, an image database and quantitative measurement framework for image texture analysis algorithms. It is not only a texture database of homogeneous texture images, but also a frame work for the quantitative measurement of texture algorithms targeted on a number of texture testing suites, and an implementation of some major well-known texture classification paradigms. The comparative study of four texture classification algorithms evaluated in the database is presented by Ohanian and Dubes [Ohanian92].

Although a number of texture sets in *MeasTex* have been compiled by other texture databases such as the *Brodatz* texture database and the *VisTex* database, most of their natural textures are 2D texture rather than 3D texture. The natural texture images are obtained from 35mm camera film, thereafter each photograph is scanned at 256dpi and stored in the database. In these cases, we do not know what the exact illumination direction is when the real texture is captured. Therefore this database is not suitable for our 3D surface classification scheme.

Another point to note about in the images of *MeasTex* is that they use direct sunlight as the lighting source in most cases, although they have made note of where the sunlight is exactly coming from. Unfortunately, our simple solution for photometric stereo cannot use these images, since the path of the sun across the sky is very nearly planar [Woodham80]. The same problem also appears in the *VisTex* database.

- ***OUTex***

OUTex stands for University of Oulu Texture database, and it is a framework for the empirical evaluation of texture classification and segmentation algorithms. At this time, the collection of 319 surface textures are captured by well defined variations to a given reference in terms of illumination directions, surface rotations and spatial resolutions. Hence given three different simulated illumination directions, six spatial resolution (100, 120, 300, 360, 500 and 600 dpi) and nine rotation angles (0° , 5° , 10° , 15° , 30° , 45° , 60° , 75° and 90°), 162 ($3 \times 6 \times 9$) images are captured from each texture sample, in both 24-bit RGB and 8-bit grey scale. Ojala and Pietikäinen [Ojala96] [Ojala98] give a comparative study of texture measures with classification based on successfully using *OUTex* database.

Compared with other texture databases such as *Brodatz*, *VisTex* and *MeasTex*, *OUTex* is comprise of a wide range of 3D texture images (162 images for each texture) taken under different illumination directions and surface orientations which potentially can be used as input images for our surface rotation invariant texture classification scheme. However, the *OUTex* database cannot used to provide registered photometric stereo data. For example, although texture images of 3D surfaces are taken under three different illumination directions in the space, all of the three involving illumination directions are lying on the same plane (coplanar or collinear), shown in *Figure 7. 1*. In the other words, all of these three illumination conditions only vary in the change of slant angle (σ), the tilt angle (τ) is constant. Therefore we can not correctly resolve the surface partial derivatives $p(x,y)$ and $q(x,y)$ from these images using photometric stereo, as the inverse of the lighting matrix in the photometric stereo solution does not exist when the three illumination vectors lie in the same plane [Woodham80] [Horn89] [Horn96] [Davies90].

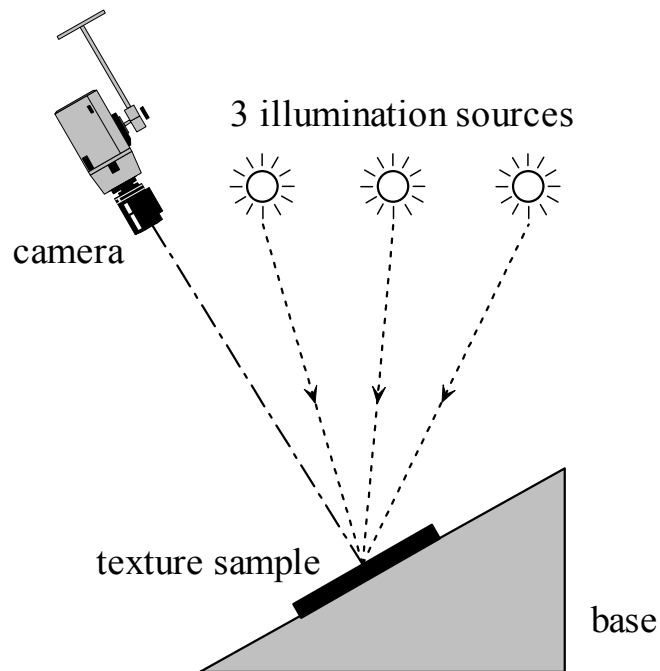


Figure 7.1 Relative positions of texture sample, illuminant and camera, used in *OUTex* database.

- ***CUReT***

Characterising the appearance of real-world surfaces is important for many computer vision algorithms. ***CUReT*** (Columbia-Utrecht Reflectance and Texture Database) developed at Columbia University and Utrecht University has collaborated in an extensive investigation of the visual appearance of real-world surfaces [Dana97] [Dana99a]. It comprises three texture databases:

- 1) ***BRDF database*** (bi-directional reflectance distribution function [Nayar91] [Wolff94]) with reflectance measurements for 61 different samples, each observed with over 205 different combinations of viewing and illumination directions,
- 2) ***BRDF parameter database*** with estimated parameters for two recent BRDF models: the Oren-Nayar model [Nayar95] [Oren95] for surfaces with isotropic roughness and the Koenderink *et al* model [Koenderink96] for both anisotropic and isotropic surfaces, and
- 3) ***BTF*** (bi-directional texture function) database. 61 real-world surfaces are measured using new texture representation called BTF. BTF describes the appearance of a textured surface as a function of the illumination and viewing

directions. Also the BTF measurement database is the first comprehensive investigation of texture appearance as a function of viewing and illumination directions [Dana99a].

They note that the appearance of real world texture is a function of both orientation of the 3D sample and the directions of viewer and illuminant. Their database combines the foreshortening effect of the texture and the associated changes in its corresponding illumination directions. For 3D textures, the BTF must also capture more complicated effects such as local shading, interreflections, and masking of surface elements. The difficulty in finding appropriate data sets for characterising BRDF and BTF of 3D texture has been resolved by the construction of *CUReT*. The set of images for each texture sample is obtained over a wide range of viewing and illumination directions.

The substantial interest in the *CUReT* database is evident in the numerous works using the database. It has been used by Dana and Nayar [Dana98] to confirm models for observed intensity distribution as a function of illumination and viewing angles. Dana and Nayar [Dana99b] describe a correlation model for 3D surface texture and suggest how this might be used to provide a 3D surface texture feature, the measured correlation length as a function of viewing direction. They do not however, use this for texture classification purposes. Suen and Healey [Suen98] [Suen00] study the properties of the dimensionality surface via analysing the Bi-directional Texture Function (BTF) using the *CUReT* database. A multi-band correlation model is used to describe image texture as a function of viewing and illumination angles. They also do not use this database for texture classification. Mäenpää and Ojala [Mäenpää00] perform an experiment using the *CUReT* database to demonstrate the robustness of texture classification in terms of changing tilt angle τ only by using local binary patterns (LBP). However, they do not involve the surface rotation as well.

Finally, we have to note that, for all measurements of a selected texture sample, the light source remains fixed. However as the camera is mounted on a tripod, with its optical axis parallel to the floor of the lab, it can be positioned to any one of seven

different locations in a plane during measurements. For each camera position and a given light source direction, the texture sample is rotated. The relative positions of texture sample, illuminant and camera used in *CUReT* database are shown in *Figure 7. 2*. The measurement setup for *CUReT* database is not suitable for photometric stereo, as for a given texture sample at a certain orientation we need to capture the different images by fixing the position of camera and moving the light source, not by fixing the light source and moving camera.

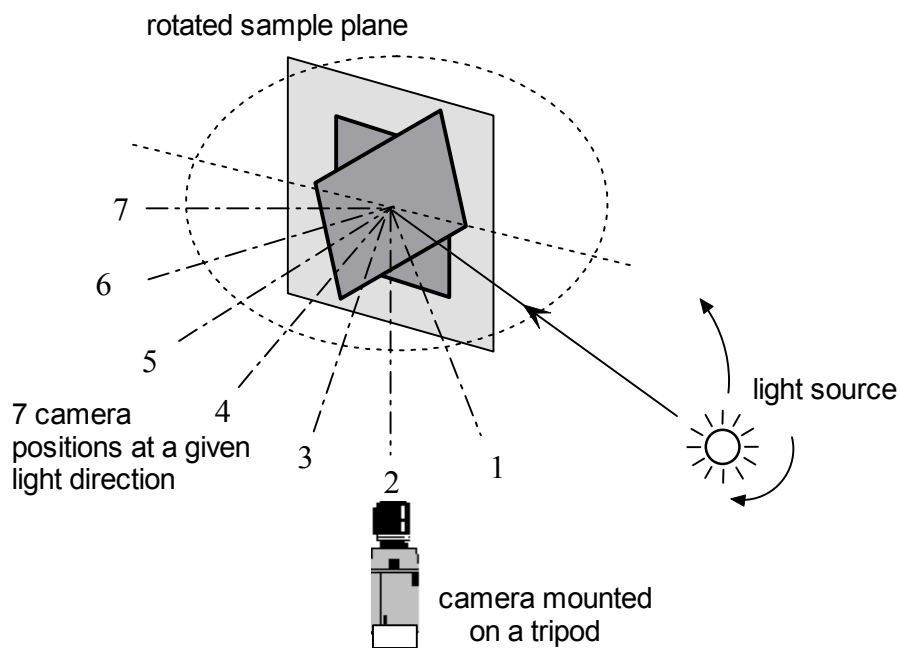


Figure 7. 2 Relative positions of texture sample, illuminant and camera, used in *CUReT* database.

- ***PhoTex Database***

PhoTex database [McGunnigle01] is a texture database of rough surface. It holds images of rough surfaces that have been illuminated from various directions. Images that allow the user to calibrated the image transfer function, and measure the noise in the process are also held in the database. The main variables in the database are azimuth and zenith of the illumination. In few cases, the surface sample is also rotated. This database therefore mainly focuses on the changes of illumination condition rather than the surface rotation. In fact, although it is a photometric texture

database that is mostly close to our requirement, it does not provide full surface rotation samples.

- **Comparative study**

Table 7. 1 summarises the properties of the texture databases that have been discussed above. It can be seen that there is no existing texture database which provides registered photometric stereo data sets.

texture database	image rotation	surface rotation	controlled illumination	registered photometric stereo
Brodatz	√	×	×	×
VisTex	√	×	√ ¹	×
MeasTex	√	×	×	×
OUTex	√	√	√	×
CUReT	√	√	√	×
PhoTex	×	×	√	√

Table 7. 1 Comparative study of existing texture databases.

7.2.3. Developing Our Photometric Texture Database

The texture due to surface roughness has complex dependencies on viewing and illumination directions. These dependencies can not be studied using those texture databases that include few images of each sample. Our texture database covers a diverse collection of rough surfaces and captures the variation of image texture with changing illumination direction. It is intended to provide photometric surface data for texture analysis (e.g. texture classification and segmentation, and 3D rough surface modelling, etc), while our task is mainly concerned with surface rotation invariant

¹ Some of them are unknown.

texture classification. There is a varied range of images of rough surfaces within the database, and the major variables are the surface orientation and the tilt angle of illumination. These provide enough information to estimate surface properties using photometric stereo. Also, we capture our images under much more constrained and controlled conditions, when compared with other texture databases available on the internet.

7.2.4. Set Up Photometric Texture Database

The first step of experimental procedure is to obtain the texture data set from the 3D surface texture. The data set consists of images captured at different rotations and illuminated from different directions. A photometric image set of each texture to be classified is captured, as shown in *Figure 7. 3*, i.e. eight images are taken at illuminant tilt angles of 0° , 45° , 90° , 135° , 180° , 225° , 270° , and 315° . Although only three of them are needed to estimate surface partial derivatives using the basic photometric stereo technique, others are needed for further investigation. The position and orientation of the surface sample will not be varied during the capture of these eight images. Each 3D texture surface is then rotated into 7 positions (surface orientation angles $\varphi = 0^\circ, 30^\circ, 60^\circ, 90^\circ, 120^\circ, 150^\circ$ and 180°). The original texture image size in the digital camera (a Vosskuhler CCD 1300LN) is set to 1280×1024 pixels. Note that the slant angle (σ) is kept as a constant of 50° during the whole experimental procedure. Thereafter, the final images are obtained by reducing them to a size of 512×512 pixels. Finally a database of 30 real textures with 1680 images ($30 \text{ textures} \times 7 \text{ rotations} \times 8 \text{ illumination directions}$) and 4 synthetic textures with 224 images ($4 \text{ textures} \times 7 \text{ rotations} \times 8 \text{ illumination directions}$) is constructed for our experiment.

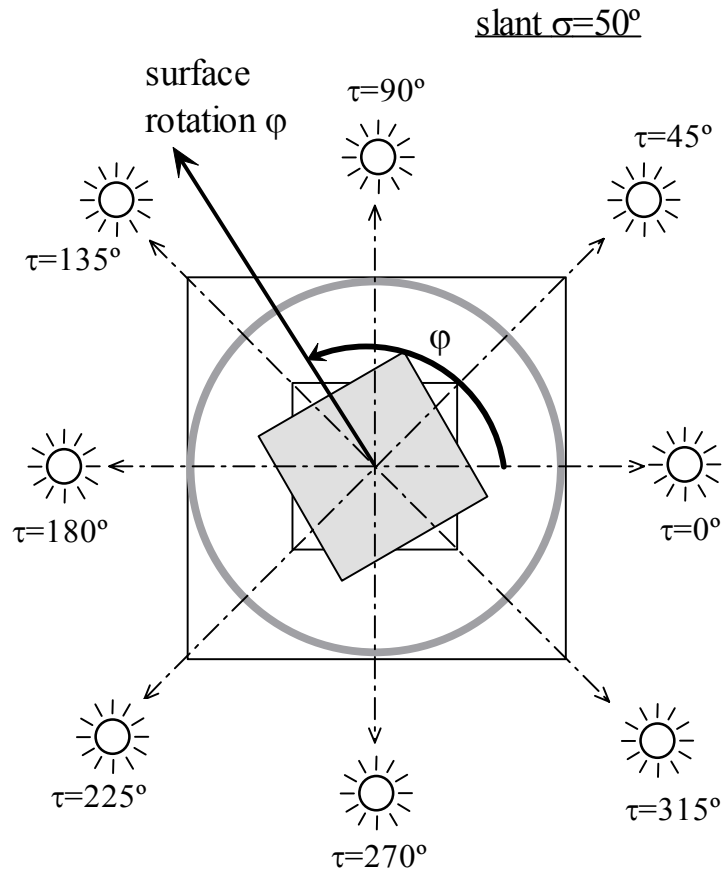


Figure 7.3 Geometry for capture of photometric image set in our experiments.

7.2.5. Texture Samples

- *Synthetic texture data set*

We refer to the synthetic textures introduced in chapter 3. Although there are only four textures in this data set, the experimental texture set contained patterns with different degrees of regularity as well as non-regular directional patterns. The montage samples of the synthetic images (*rock*, *sand*, *ogil malv*) at different surface orientations are shown in Figure 7.4.

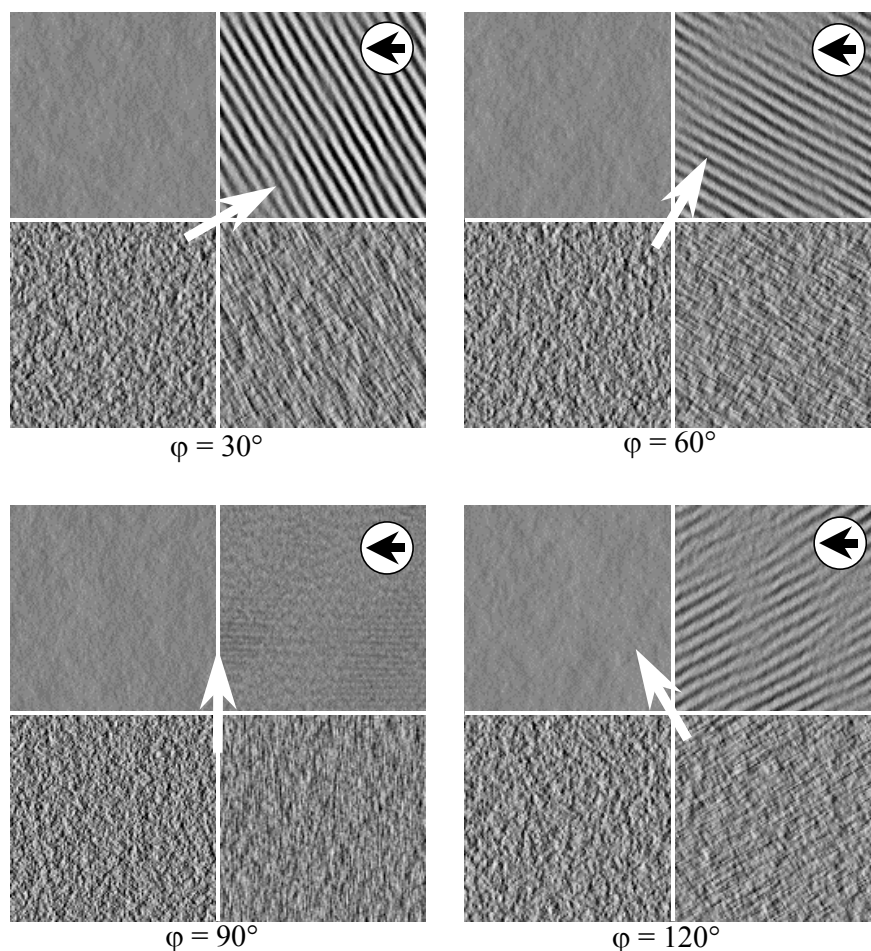


Figure 7.4 Four synthetic textures at four surface rotations ($\varphi = 30^\circ$, 60° , 90° , and 120°) with constant illumination (slant $\sigma = 50^\circ$). Surfaces are generated synthetically, rotated as indicated by white arrows in the centre, rendered using Lambert's law at an illuminant tilt of $\tau=0^\circ$ as indicated black arrows in white circles and combined into montage format for display purposes. (rock on left top, sand on right top, malv on left bottom and ogil on right bottom).

- **Real texture data set**

There is a great diversity of textures for a real world scene (micro-textures and macro-textures), and consequently of texture classification problems. For example, textures can be as diverse as landmarks, forests and oceans viewed from space, different kinds of textiles, clothes, rock, patterns of photographs on a flat surface, any homogenous region that can be seen as an image [Graham70]. On the other hand, we are interested in texture features such as directionality, periodicity, randomness, roughness, regularity, coarseness, albedo distribution, contrast and complexity,

which are hypothesised to be important for human perception an attention [Tamura78]. This real texture data set is focused on the use of collective visual properties or vision textures, shown in *Figure 7. 5*.

The samples are chosen from the wide range of physical surfaces, including isotropic surfaces (*gr2*), directional surfaces (*tl5*), bi-directional surfaces (*tl4*), multi-directional surfaces (*tl2*), specula surfaces (*wps2*), heavy-shadowed surfaces (*rkb1*), surfaces with small height variations (*grd1*), surfaces with large height variations (*bn1*), and so on. The materials include textile, corduroy, terry, bean, wallpaper, plaster, rock, noodle, wood, concrete, styrofoam, etc.

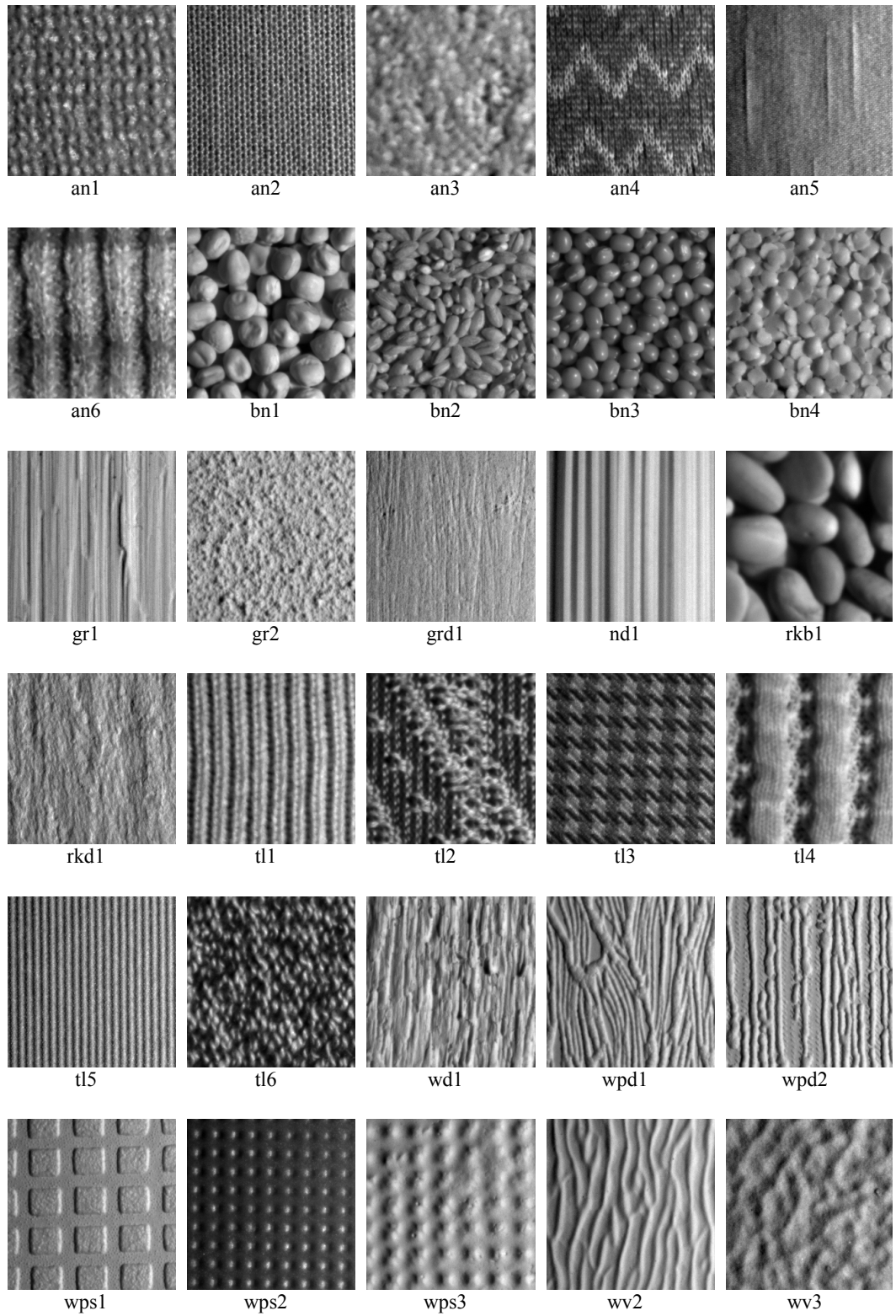


Figure 7.5 30 real texture samples at surface rotations $\varphi = 0^\circ$ under the illuminant condition of slant $\sigma = 50^\circ$ and tilt of $\tau=0^\circ$. (image size 256×256)

7.3. Settings of the Experimental Apparatus

Experimental apparatus was constructed for the acquisition of images under controlled lighting conditions. All of the imaging facilities were placed in a dark room, and an overview of the layout of the system is shown in *Figure 7. 6* and *Figure 7. 7*, followed by a detailed discussion of significant design aspects.

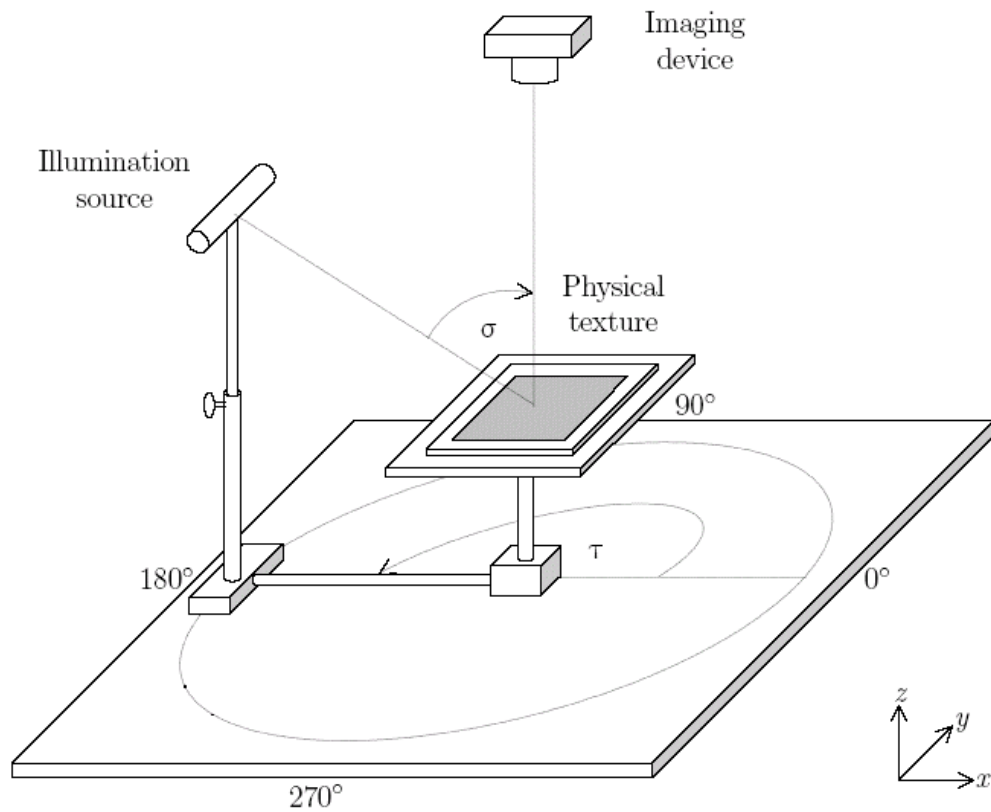


Figure 7. 6 . Laboratory apparatus to collect photometric stereo image data.

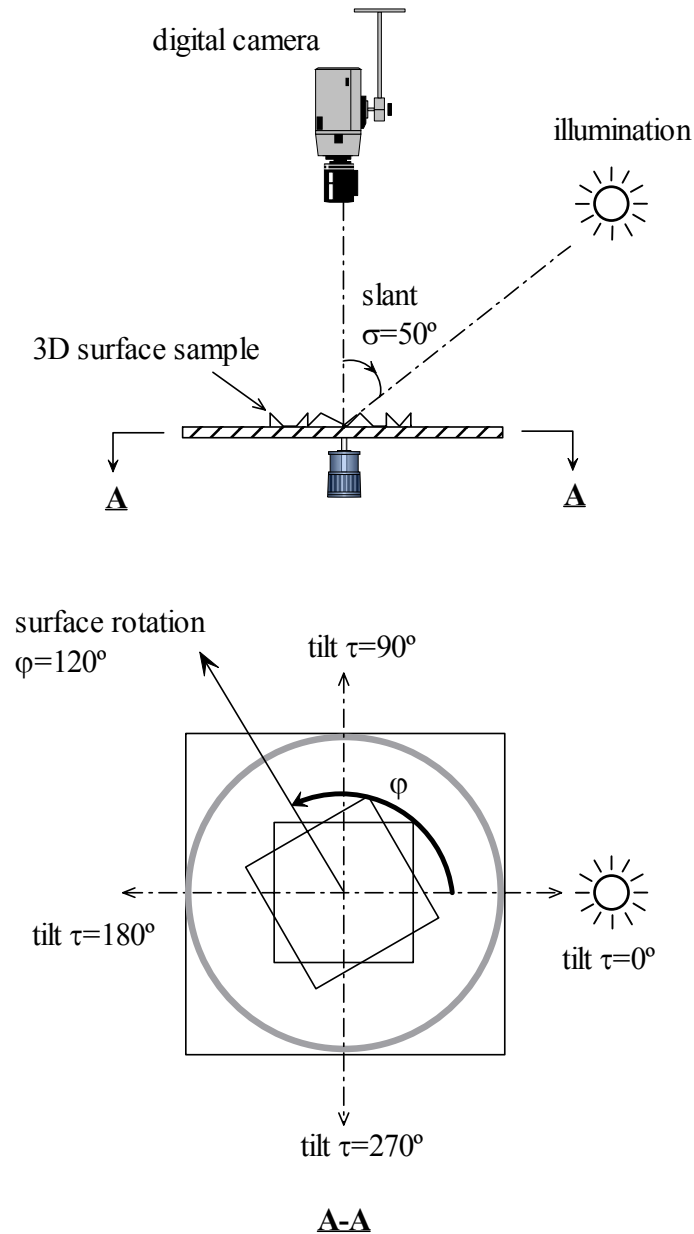


Figure 7. 7 Geometry of the surface capturing system

We mount the CCD camera directly overhead the testing sample and put the 3D surface texture sample on a rotated plane. Apart from the rotation variance, our system can cope with changes in illumination conditions (i.e. changes of tilt angle (τ) and slant angle (σ)). The image is captured by an overhead digital camera and illuminated by a light source with slant angle (σ) and tilt angle (τ). The multiple images required for photometric stereo can be obtained by explicitly moving a single light source arm. The illumination direction (σ and τ) can be adjusted manually. In

our experiment, the slant angle (σ) is kept as a constant of 50° during the whole experimental procedure.

- ***Digital Camera***

The digital camera used in our experiments is a CCD-1300LN made by VDS Vosskühler (<http://www.vdsvossk.de>). It is used with a Matrox PC-SIG framestore with a resolution of $1280(\text{height}) \times 1024(\text{width})$ effective pixels. Pixel size is $6.7\mu\text{m} \times 6.7\mu\text{m}$. The RS-644 digital output supplies images data with *12-bit* precision in uncompressed grey-level TIFF format.

The camera aperture is fixed at one setting for all data capture. This helps to keep the linear relationship between pixels and radiance, specially in the range between low and high radiance values, as pixel underflow and overflow, i.e. pixels which are clipped into values of 0 or 4095 by digitisation (*12-bit*), contribute significantly to non-linearity.

- ***Light Source***

The single light device is powered by a stabilised DC supply and mounted on a rotated arm which can be moved to the specified tilt and slant angle. Thus selecting the illumination directions over the hemisphere of possible directions can be achieved manually. The light source is a filament tube with a mask, which provides a Gaussian spatial distribution of illumination. The time varying component of the image, photon noise is associated with the quantum nature of light in [Healey94]. In order to assess the stability of the light source (e.g. spatial uniformity and non-time-varying), we measure the light intensity via a digital light meter (*Lux-Meter 0560 in standard DIN 5035*). The *Lux-Meter* was a useful measuring instrument for ensuring that the illumination was kept at a constant 65 Lux for each texture.

7.4. Experimental Procedure

In this section, we will outline the experiment procedure in four main steps in order to demonstrate our surface rotation invariant texture classification scheme: set up photometric texture database; partitioning the training and testing textures; extracting features and classification.

7.4.1. Partitioning the Training and Test Textures

- *Using Over-lapping Textures*

For our classification system, the data are partitioned into training and test sets respectively. Training is performed using photometric image sets with the surfaces obtained at a surface rotation angle of $\varphi = 0^\circ$, and the size of training images is set to 512×512 pixels. The test textures are obtained by using separate sample with rotations at 30° increments over the range from 30° to 180° . This partition strategy will give us a blind classification scheme.

In order to increase the number of classifications tests, each of the photometric sets was divided into nine smaller over-lapping photometric sets, in which each image has the size of 256×256 pixels, illustrated in *Figure 7. 8*. This gave a total of 4860 ($30 \text{ textures} \times 3 \text{ photometric stereo images} \times 6 \text{ rotations} \times 9 \text{ subimages}$) photometric test samples. *Table 7. 2* summarises the partition strategy of training and test textures.

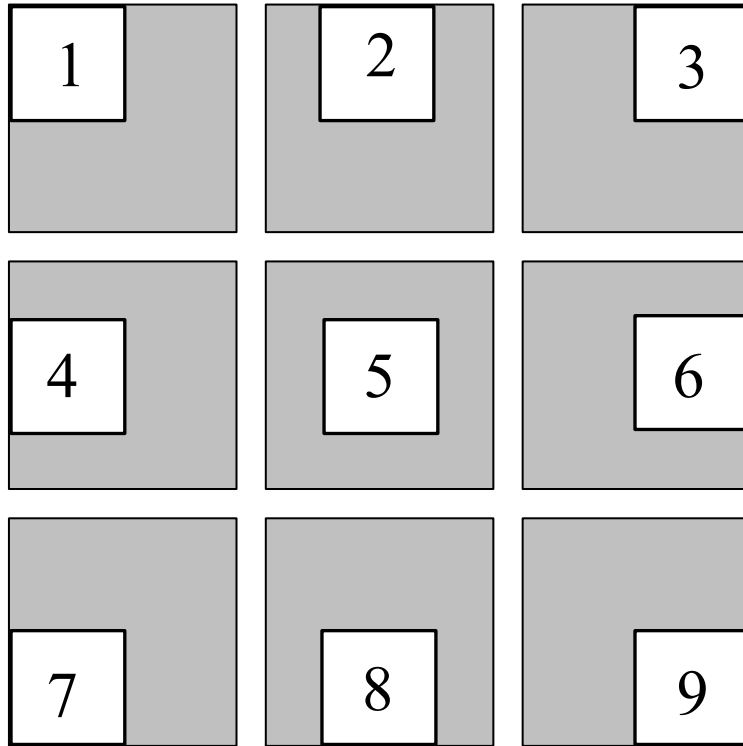


Figure 7. 8 Illustration of positions of the 9 over-lapping test 256×256 images obtained from a single 512×512 image.

		Training textures	Test textures
Surface orientation φ		0°	$30^\circ, 60^\circ, 90^\circ, 120^\circ, 150^\circ$ and 180°
Image size		512×512	256×256
Number of textures	Synthetic	4	
	Real	30	
Number of images	Synthetic	$4 \times 3 = 12$	$4 \times 3 \times 6 \times 9 = 648$
	Real	$30 \times 3 = 90$	$30 \times 3 \times 6 \times 9 = 4860$
Number of classifications	Synthetic	$4 \times 6 \times 9 = 216$	
	Real	$30 \times 6 \times 9 = 1620$	

Table 7. 2 Summary of partitioning of training and test textures using over-lapping textures.

- **Using Non-overlapping Textures**

Figure 7. 9 and Table 7. 3 show the strategy of partitioning of training and test textures using non-overlapping textures.

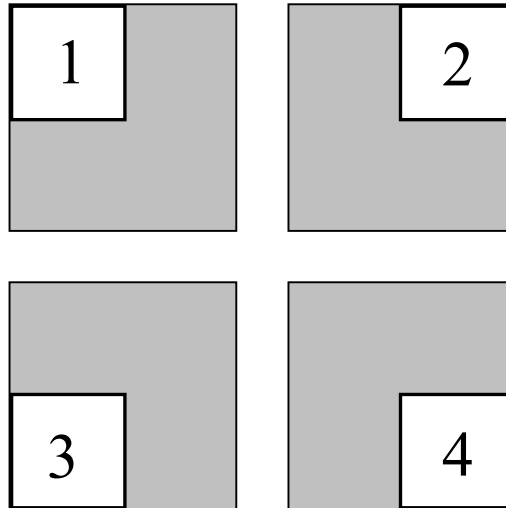


Figure 7. 9 Illustration of positions of the 4 non-overlapping test 256x256 images obtained from a single 512x512 image.

		Training textures	Test textures
Surface orientation φ		0°	$30^\circ, 60^\circ, 90^\circ, 120^\circ, 150^\circ$ and 180°
Image size		512×512	256×256
Number of textures	Synthetic	4	
	Real	30	
Number of images	Synthetic	$4 \times 3 = 12$	$4 \times 3 \times 6 \times 4 = 288$
	Real	$30 \times 3 = 90$	$30 \times 3 \times 6 \times 4 = 2160$
Number of classifications	Synthetic	$4 \times 6 \times 4 = 96$	
	Real	$30 \times 6 \times 4 = 720$	

Table 7. 3 Summary of partitioning of training and test textures using non-overlapping textures.

7.4.2. Extracting Features

1. The photometric algorithm uses this image set to estimate the surface partial derivatives $p(x,y)$ and $q(x,y)$.
2. These are Fourier transformed and processed to provide gradient spectra $M(\omega, \theta)$ and polar spectrum $\Pi(\theta)$. The variance of the coefficients and the spectral leakage introduced by a standard FFT are reduced by using a Welch periodogram [Welch67] coupled with a circular Hann window. The principle of 2-D Welch periodogram is take a series of overlapping, smaller 2-D Hanning windows in the image, the FFT for each of these windows is calculated and finally the results are obtained by averaging across FFT. This reduces the variance of the power estimate by averaging over all the windows, which leads to a general smoothing of the final spectrum.
3. The polar spectrum of the test texture is compared with the polar spectrum obtained from training images over a range of angular displacements φ_{test} using a sum of squared differences metric. The experiments based on synthetic textures and real textures are designed to show that the gradient spectra $M(\omega, \theta)$ functions and their polar spectrums are rotationally sensitive but contain no directional artefacts. That is $M_\varphi(\theta) = M(\theta + \varphi)$ and similarly $\Pi_\varphi(\theta) = \Pi(\theta + \varphi)$.

7.4.3. Classification

In the classification process, the similarity between the training and test data sets are measured with SSD and the testing sample is assigned to the class. The total sum of squared errors statistic is calculated from polar spectrums and the best combination provides a classification decision and an estimation of the relative orientation of the

test texture. The test polar spectrum must be “rotated” (or rather translated) to find the best-fit. The texture is then assigned to the class for which the lowest sum of square differences occurs at each of these best-fit rotation angles. The classification experiments are performed on both synthetic and real texture data sets, respectively.

In terms of the classification using over-lapping texture images, each of the resulting 1620 ($30 \text{ textures} \times 6 \text{ rotations} \times 9 \text{ subimages}$) polar spectrums is compared with each of the 30 'training' polar spectrums in the database of real textures; while each of the resulting 216 ($4 \text{ textures} \times 6 \text{ rotations} \times 9 \text{ subimages}$) polar spectrums is compared with each of the 4 “training” polar spectrums in the database of synthetic textures.

On the other hand, in terms of the classification using non-overlapping texture images, each of the resulting 720 ($30 \text{ textures} \times 6 \text{ rotations} \times 4 \text{ subimages}$) polar spectrums is compared with each of the 30 'training' polar spectrums in the database of real textures; while each of the resulting 96 ($4 \text{ textures} \times 6 \text{ rotations} \times 4 \text{ subimages}$) polar spectrums is compared with each of the 4 “training” polar spectrums in the database of synthetic textures.

7.5. Presentation of Experimental Results

Note that the classification results presented on the following chapters in this thesis are based on the over-lapping textures for both training and test data set unless it is indicated.

7.5.1. Synthetic Textures

- ***Classification Results by Using Over-lapping Synthetic Texture Images***

For our synthetic texture data set, we achieve perfect classification accuracy of 100% . Some of examples of sum of squared difference (SSD) metrics between the

training textures (at surface orientation $\varphi = 0^\circ$) and test textures (at orientations $\varphi = 30^\circ, 60^\circ, 90^\circ$, and 120°) are shown in Table 7. 4. We note that, the classification performs well whatever the orientation of the test data. The minimal value of SSD (indicated by the grey colour background in the table) is only achieved between the polar spectrum of the test texture and their OWN training polar spectrum, although the orientation of the test polar spectrum is different from that of training polar spectrum. Hence, our classification scheme is rotation-invariant for these textures.

Training->	rock_ref0	sand_ref0	ogil_ref0	malv_ref0
Rotation $\varphi = 30^\circ$ (testing)				
rock_30	5.83E-01	2.99E+05	1.67E+04	1.65E+04
sand_30	5.42E+05	6.11E+04	4.51E+05	5.14E+05
ogil_30	1.19E+04	2.42E+05	7.52E+02	5.66E+03
malv_30	1.45E+04	2.79E+05	6.81E+03	3.36E+02
Rotation $\varphi = 60^\circ$ (testing)				
rock_60	5.12E-01	2.99E+05	1.67E+04	1.65E+04
sand_60	6.09E+05	1.24E+05	5.27E+05	5.85E+05
ogil_60	1.10E+04	2.40E+05	9.38E+02	5.59E+03
malv_60	1.33E+04	2.81E+05	6.62E+03	4.54E+02
Rotation $\varphi = 90^\circ$ (testing)				
rock_90	8.35E-02	2.99E+05	1.66E+04	1.64E+04
sand_90	2.31E+05	2.50E+04	1.73E+05	2.16E+05
ogil_90	1.69E+04	2.28E+05	3.15E+02	7.11E+03
malv_90	1.69E+04	2.79E+05	7.11E+03	1.22E+02
Rotation $\varphi = 120^\circ$ (testing)				
rock_120	7.10E-01	2.99E+05	1.67E+04	1.66E+04
sand_120	5.45E+05	6.21E+04	4.53E+05	5.17E+05
ogil_120	1.18E+04	2.42E+05	7.60E+02	5.69E+03
malv_120	1.31E+04	2.79E+05	6.58E+03	4.55E+02

Table 7. 4 Sum of squared difference metric values between the training textures (at the surface orientation of $\varphi = 30^\circ, 60^\circ, 90^\circ$, and 120°) and test textures (at the surface orientation of $\varphi = 0^\circ$) for four synthetic textures (rock, sand, ogil and malv).

We note that the minimal values of SSD (indicated by the grey colour background) in Table 7. 4 are still high apart from texture “rock”. This is due to consideration of that our training data are rotated surfaces rather than image rotation which involve much more noises.

- ***Effect of Sample Size by Using Non-overlapping Synthetic Texture Images***

In these experiments with synthetic textures good performance (100% classification accuracy) was achieved using relatively large samples with a size of 256×256 pixels. In order to show the effect of image size against the classification accuracy, the experiment was repeated using test sample sizes of 128×128 , 64×64 , and 32×32 pixels. Consequently, all of the smaller samples are cut from the original 512×512 images to provide the maximum number of samples without overlapping. Thus for example, in the case of test image size of 32×32 , 6144 classifications were performed ($4 \text{ textures} \times 6 \text{ rotations} \times 256 \text{ samples per rotation}$). The classification results are shown below in *Table 7. 5* and *Figure 7. 10*.

Testing sample size	256×256	128×128	64×64	32×32
Number of samples per rotation	9	16	64	256
	Overlapped	Non-overlapped		
Number of classification	$4 \times 6 \times 9 = 216$	$4 \times 6 \times 16 = 384$	$4 \times 6 \times 64 = 1536$	$4 \times 6 \times 256 = 6144$
Misclassification rate	0%	8%	21%	32%

Table 7. 5 Classification results for 4 synthetic textures with the different testing sample size.

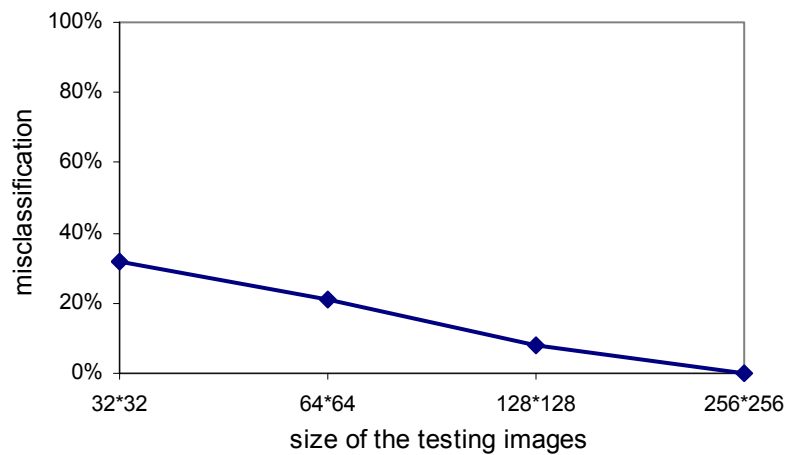


Figure 7. 10 Misclassification rate for 4 synthetic textures against the size of the test samples.

As expected, the results show that this approach is sensitive to the test sample size.

- **Surface-based Texture Classification vs. Image-based Texture Classification**

Firstly, *Table 7. 6* summarises the partitioning of training and test textures used in image-based texture classification scheme (presented in *Figure 6.23*). This gives a total number of 216 ($4 \text{ textures} \times 6 \text{ rotations} \times 9 \text{ subimages}$) classifications. On the other hand, the strategy of partitioning for surface-based texture classification scheme (presented in *Figure 6.22*) can be referred back to *Table 7. 2*.

	Training textures	Test textures
Surface orientation φ	0°	$30^\circ, 60^\circ, 90^\circ, 120^\circ, 150^\circ \text{ and } 180^\circ$
Image size	512×512	256×256
Number of textures	4	
Number of images	4	$4 \times 6 \times 9 = 216$
Number of classifications	$4 \times 6 \times 9 = 216$	

Table 7. 6 Summary of partitioning of training and test textures used in image-based texture classification scheme for synthetic textures.

Secondly, the classification accuracy for image-based classifier is shown in *Table 7. 7*, compared with those for surface-based classifier. Note that the classification performance of image-based classifier is worse than that of surface-based classifier. In addition, in terms of image-based classification, the isotropic textures “rock”(81.5%) and “malv”(92.6%) have better classification accuracies than directional textures “sand”(37.0%) and “ogil” (55.6%). This can be explained by the fact of that the directional illumination filter effects on the directional 3D surfaces. Classifier only using image information loses the information about the directionalities of 3D surfaces.

	<i>rock</i>	<i>sand</i>	<i>malv</i>	<i>ogil</i>
Surface-based	100%	100%	100%	100%
Image-based	81.5%	37.0%	92.6%	55.6%

Table 7. 7 Classification accuracy for 4 synthetic textures: image-based classifier vs surface-based classifier.

7.5.2. Real Textures

- *Classification Results by Using Over-lapping Real Texture Images*

An average recognition rate of 76.30% was obtained for 30 real textures. Classification results for each of the real texture classes are shown in *Figure 7. 11*.

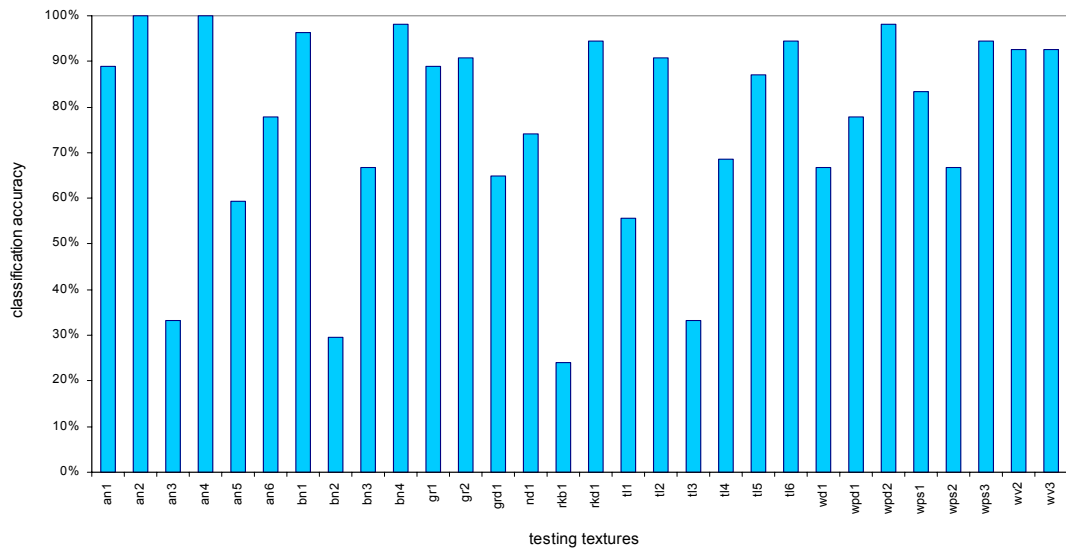


Figure 7. 11 Classification results for 30 real textures by using over-lapping texture images.

Comments on results can be summarised as followings:

1. The misclassifications may well be due to shadows and non-Lambertian surfaces – both of these factors cause the photometric stereo to introduce errors (e.g. a classification accuracy of 24.07% is obtained with the heavily shadowed texture “*rkb1*”).

2. The results of classification accuracy for each individual texture show that our classification scheme performs better with directional textures than isotropic textures. For example, three of the four worst classification results are caused by isotropic textures (“*rkb1*” with 24.07%, “*bn2*” with 29.63% and “*an3*” with 33.33%).

- ***Classification Results by Using Non-overlapping Real Texture Images***

Figure 7. 12 shows the classification results for 30 real textures by using non-overlapping images. The strategy of partitioning of non-overlapping images can be referred back to *Figure 7. 9*. In addition, the number of training and test images and the number of classifications has been summarised in *Table 7. 3*.

The overall classification accuracy is 78.5% by using non-overlapping texture images, which is a little better than that of 76.30% by using over-lapping texture images (*Figure 7. 11*). However, those two overall classification accuracies for 30 real textures between using non-overlapping images and using over-lapping images are not comparative. The reason of this case is that they share the same training data set (see *Table 7. 2* and *Table 7. 3*), while the test data set using non-overlapping images is only the sub-set of the test data set using over-lapping images. On the other hand, the classification number using non-overlapping is reduced from 54 ($6 \text{ rotations} \times 9 \text{ subimages}$) to 24 ($6 \text{ rotations} \times 4 \text{ subimages}$) for each texture class, which also results in that the total number of classifications is reduced from 1620 to 720 (see *Table 7. 2* and *Table 7. 3*). Therefore, we cannot compare those two classifications that have the different test data sets.

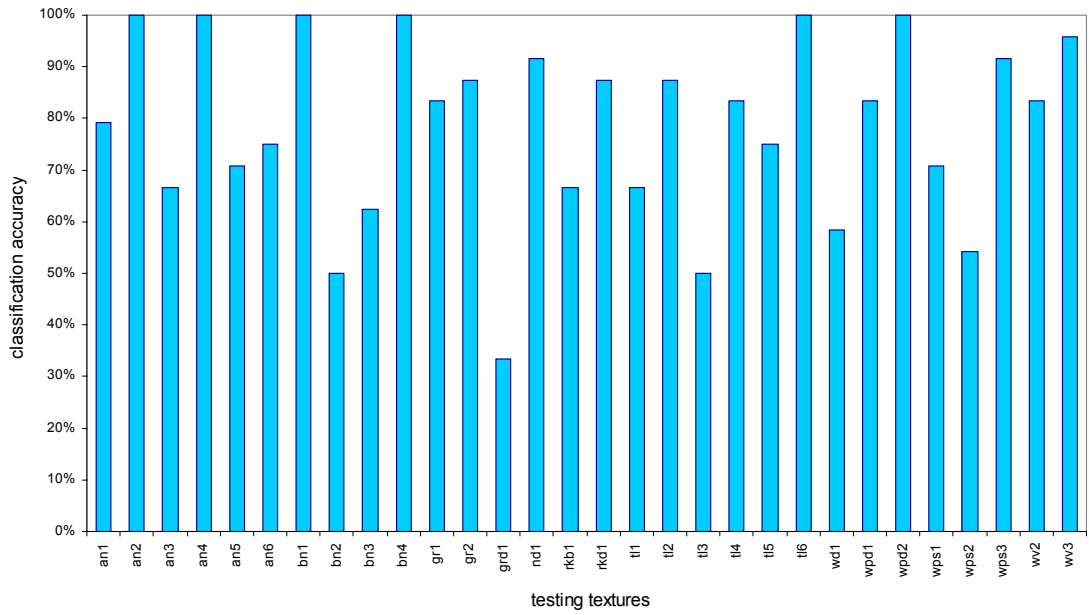


Figure 7.12 Classification results for 30 real textures by using non-overlapping texture images.

- **Surface-based Texture Classification vs. Image-based Texture Classification**

Now we carry out the similar comparative studies on real textures in the same way as we do on synthetic textures. Table 7.8 summarises the partitioning of training and test textures used in image-based texture classification scheme (presented in Figure 6.23). This gives a total number of 1620 ($30 \text{ textures} \times 6 \text{ rotations} \times 9 \text{ subimages}$) classifications.

	Training textures	Test textures
Surface orientation φ	0°	$30^\circ, 60^\circ, 90^\circ, 120^\circ, 150^\circ \text{ and } 180^\circ$
Image size	512×512	256×256
Number of textures	30	
Number of images	30	$30 \times 6 \times 9 = 1620$
Number of classifications	$30 \times 6 \times 9 = 1620$	

Table 7.8 Summary of partitioning of training and test textures used in image-based texture classification scheme for real textures.

Figure 7.13 shows the classification results for 30 real textures between image-based classifier and surface-based classifier. The overall classification accuracy of

29.2% for image-based classifier is much worse than that of 76.3% for surface-based classifier. It also proves that 3D surface rotation is not the same as the 2D image rotation. Rotation of the physical texture surface under fixed illumination conditions can cause significant changes to its appearance, and cause failure of classifiers designed to copy with image rotation.

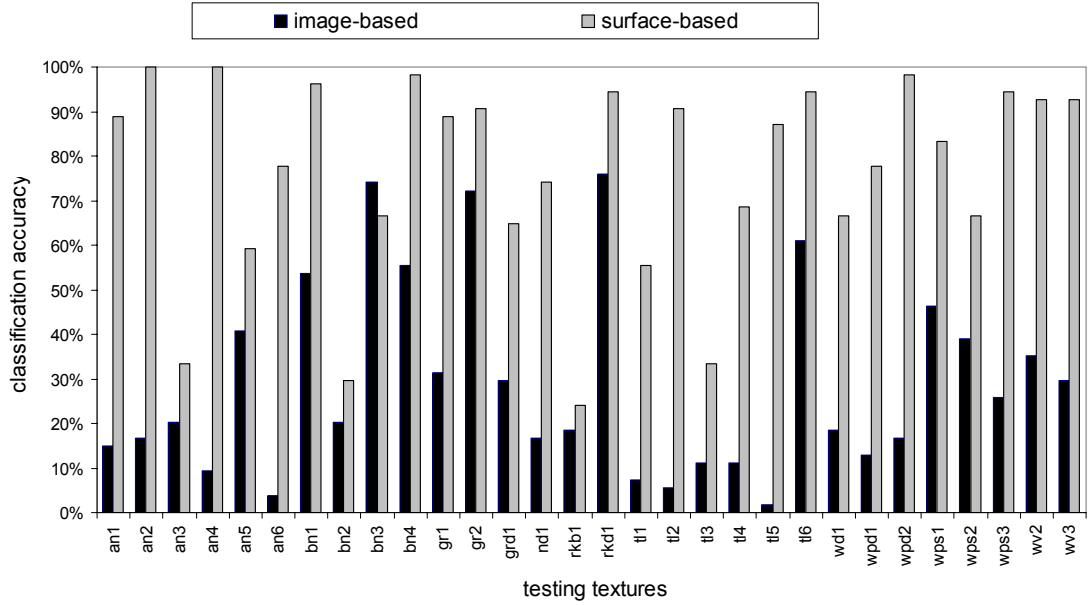


Figure 7.13 Classification results for 30 real textures: image-based classifier vs surface-based classifier.

7.5.3. Comparative Study on Other State-of-the-art Approaches

In this section, our algorithm is compared to those of Leung and Malik [Leung99], Varma and Zisserman [Varma02a], which are the current state-of-the-art approaches. The tests [Varma02b] on both algorithms are using our photometric texture database.

- **Leung and Malik's Method**

Leung and Malik [Leung99] make an important innovation in giving an operational definition of a *texton*. The main idea is to construct a vocabulary of prototype tiny surface patches with associated local geometric and photometric properties. They call

those *3D textons*. They make a serious attempt on the problem of classifying textures under varying viewpoint and illumination. Their solution was a *3D texton* which is a cluster centre of filter responses over a stack of images with representative viewpoints and lighting.

- ***Varma and Zisserman's Method***

Varma and Zisserman [Varma02a] present an approach to material classification under unknown viewpoint and illumination. Their texture model is based on the statistical distribution of clustered filter responses. However, unlike previous *3D texton* representations [Leung99], they use rotationally invariant filters and clusters in an extremely low dimensional space. Their approach to the classification problem is to model a texture as a distribution over textons, and learn the textons and texture models from training images. Classification of a novel image then proceeds by mapping the image to a texton distribution and comparing this distribution to the learnt model.

We therefore investigate Varma and Zisserman's method and implementation [Varma02b] along the comparative studies to our algorithms. The overview of their algorithm is as follows:

- ❖ **Learning Phase**

1. Take all the training images of a given texture class and filter them using given filter-bank.
2. Vector quantizes all the filter responses, across all texture classes, into textons using the *K-Means* clustering algorithm.
3. To each filter response, associate the texton which lies closest to it in filter response space.
4. The texture model for a given training image then becomes the histogram of texton labelling for that training image.
5. The texture model for a class is the set of models generated by all the training images for that class.

❖ Classification Phase

1. Given a single novel image to classify, filter it using the same filter bank and then label it using the textons that were generated in the learning phase.
2. Construct the histogram of texton labelling for the novel image.
3. Using the χ^2 metric as a distance function, determine the training model closest to the novel image histogram. Report the novel image as belonging to the same texture class as the training model (i.e. use a nearest neighbour classifier).

❖ Implementation Details

1. All 56 (7 surface rotations by 8 illumination rotations) images per texture were used. 28 were used for training and 28 for testing.
2. All the images were sub-sampled into 256×256 pixels.
3. Also, all the pre and post processing steps described [Varma02a] were implemented. The MR8 filter bank was used.
4. Again, 10 textons were learnt from each texture class to make a total of 300 textons.

❖ Classification Results

All the 840 (30 textures by 7 surface rotations by 4 illumination rotations) test images were classified correctly.

It is also reported that the classification accuracy of 100% is achieved by both two algorithms on our photometric texture database [Varma02b]. Compared with our classification accuracy of 76.30% on the same texture database at this stage, further investigation must be carried out to address this matter. In the next two chapters, we will give details of the misclassifications, and present the new classification schemes which overcome these problems.

7.6. Summary

In this chapter we presented the experimental procedure and results for a surface rotation invariant texture classification scheme. The experiments are performed using four synthetic textures and thirty real textures. For each texture, images at different surface orientations and under controlled illumination conditions are classified. We assume we have three frontal-parallel views of the test and training textures obtained under three different, known illumination conditions. We should also point out that the three-image photometric stereo algorithm used in these experiments assumes that the surfaces are Lambertian and shadow free.

Experiment results are obtained with both synthetic and real textures, where the classifier is trained at one particular rotation angle and tested with samples from other rotation angles. Our results using four synthetic textures show that our classification scheme is able to provide a successful classification rate of *100%*. A average classification accuracy of *76.30%* is obtained when thirty real textures were used. We also, note that, our classification scheme achieves good classification rates using large sample sizes and poorer classification rates using smaller sizes. While the results using real textures are not as high as those published for some image rotation invariant schemes [Cohen91] [Reed93] [Hayley96] [Port97] [Fountain98] [Zhang02a], they are good considering the difficulties involved with the rotation of real 3D surface textures and the large number of different texture classes presented.

In the next two chapters, we will give details of the misclassifications, and explain why they are happening, and present the new classification schemes which overcome these problems.